

# Stress-Induced Martensitic Phase Transformation in Intermetallic Nickel Aluminum Nanowires

Harold S. Park\*

*Department of Civil and Environmental Engineering, Vanderbilt University,  
Nashville, Tennessee 37235*

*Received January 5, 2006; Revised Manuscript Received February 24, 2006*

## ABSTRACT

Atomistic simulations are utilized to demonstrate a stress-induced martensitic phase transformation in intermetallic nickel aluminum (NiAl) nanowires. The martensitic phase transformation occurs by the propagation and annihilation of  $\{101\}$  twinning planes and transforms the initially B2 NiAl nanowires to a body-centered tetragonal (BCT) phase. The instability of the resulting BCT phase allows pseudoelastic recovery of inelastic strains on the order of 40% at all deformation temperatures.

The discovery of multifunctional materials has consistently led to the development of smaller, stronger, and increasingly versatile machines and devices. With the current emphasis on the development and utilization of active and sustainable nanotechnologies, the search for nanomaterials that exhibit combinations of desirable properties such as high mechanical strength, reversible inelastic deformation, fatigue resistance, and the ability to act as a sensor or actuator has exploded in recent years.

Nanowires are one nanoscale structural element that has shown such multifunctional potential and thus have been the focus of intense research for the past decade due to their incredible mechanical, electrical, and thermal properties resulting from their nanometer size scales.<sup>1,2</sup> These unique properties result from the fact that surface stresses and the crystallographic orientation of surfaces play a dominant role in characterizing material properties at the nanoscale. In terms of mechanical behavior, the effects of intrinsic surface stresses<sup>3</sup> have been found to endow nanowires with extremely high yield stresses and strains<sup>4,5</sup> as well as yield strength asymmetry in tension and compression;<sup>6</sup> crystallographic side surface orientation has also been found to have a direct, first-order effect on the deformation mode seen in face-centered cubic (FCC) nanowires.<sup>7</sup>

Recently, molecular dynamics (MD) simulations have shown that surface stresses contribute heavily to structural reorientations and phase transformations in metal nanowires. For example, a surface-stress-driven phase transformation from FCC to body-centered tetragonal (BCT) was observed in gold nanowires by Diao et al.<sup>8</sup> More recently, novel shape

memory and pseudoelastic behavior was observed in single-crystalline, monatomic FCC nanowires.<sup>9–11</sup> The shape memory and pseudoelasticity operates via a reversible reorientation between a lower energy  $\langle 110 \rangle$  orientation with a rhombic cross section and  $\{111\}$  side surfaces and a higher-energy  $\langle 100 \rangle$  orientation through reversible twin propagation and annihilation. This shape memory effect implies that metal nanowires may be utilized in the future as advanced nanoscale structural materials and elements.

In this letter, we demonstrate that intermetallic nanowires also show such multifunctional potential by undergoing stress-induced martensitic phase transformations. Bulk NiAl has been extensively studied<sup>12–14</sup> due to its excellent thermal conductivity, high-temperature strength, and high melting point and because it shows the shape memory effect.<sup>15,16</sup> These properties have generated much interest in using NiAl alloys as a high-temperature structural materials. Unfortunately, single-crystalline NiAl has been found to be quite brittle and exhibit limited tensile ductility, while having reduced strength at higher temperatures.<sup>12</sup>

In contrast, intermetallic NiAl nanowires can undergo a stress-induced martensitic phase transformation from an initially B2 phase to a BCT phase. The phase transformation occurs across a wide range of deformation temperatures and results in fracture strains approaching the theoretically predicted maximum for an initially B2 lattice.<sup>17</sup> The ductility of the NiAl nanowires is illustrated by the fact that the recoverable inelastic tensile strain is on the order of 40%, thus greatly outperforming both bulk NiAl<sup>16</sup> as well as commonly used shape memory alloys (SMAs) such as NiTi.<sup>18</sup> While the martensitic phase transformation in NiAl has been studied using MD by various researchers,<sup>17,19–22</sup> we dem-

\* Author to whom correspondence should be addressed. E-mail: harold.park@vanderbilt.edu.

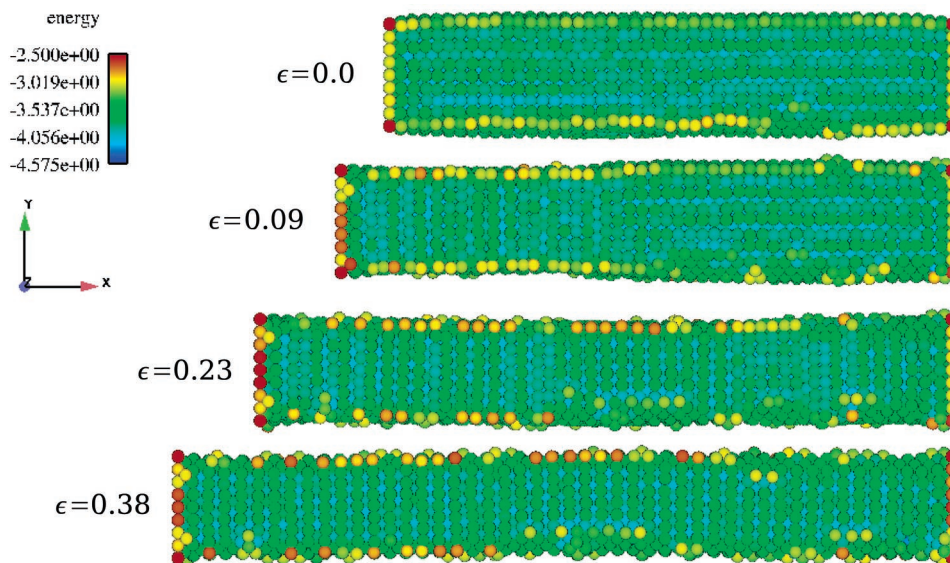


**Figure 1.** Stress-induced phase transformation from B2 to BCT in a NiAl nanowire at 350 K.

onstrate this effect in nanowires for the first time as well as the instability of the resulting BCT phase, which leads to pseudoelastic recovery of inelastic strains at all deformation temperatures.

**Methods.** The alloyed NiAl nanowires were created by generating atomic positions as in the bulk corresponding to the B2 crystal structure, which is equivalent to a body-centered cubic (BCC) lattice with the Ni atoms at the corners of the unit cell and a single Al atom at the body center. The NiAl nanowire considered consisted of 7041 atoms, with Ni atoms exclusively on the wire surfaces. The lattice constant of the B2 structure was 0.28712 nm, leading to wire lengths of 13.6325 nm in the  $x$ -direction and 2.296 nm in the  $y$ - and  $z$ -directions. The NiAl alloy was modeled using the potential of Voter and Chen, which has been utilized to study surface relaxation in Ni, Al, NiAl, and Ni<sub>3</sub>Al.<sup>23,24</sup> The potential was fit to the lattice constant, cohesive energy, elastic constants, ordering energy, vacancy formation energy, {111} and {100} antiphase boundary energies, and the super intrinsic stacking fault energy of L1<sub>2</sub> Ni<sub>3</sub>Al as well as the lattice constant and cohesive energy of B2 NiAl. Off-stoichiometric compositions of NiAl, which have been utilized to increase the yield strength and hardening<sup>12</sup> are not considered in this work.

The NiAl nanowire was first relaxed to energy-minimizing positions while keeping the ends of the wire constrained to move in the  $\langle 100 \rangle$ , or  $x$ -direction, then thermally equilibrated to four different temperatures, 50, 350, 650, and 950 K, using a Nosé–Hoover thermostat.<sup>25,26</sup> The wires were then loaded in tension in the  $\langle 100 \rangle$  direction by fixing one end of the wire and applying a ramp velocity that went from zero at the fixed end to a maximum at the loading end; the applied tensile strain rate was  $\dot{\epsilon} = 3.4 \times 10^9 \text{ s}^{-1}$ . The purpose of the initial ramp velocity was to mitigate effects from shock loading that can occur in dynamic loading conditions. Both the loading and the unloading results shown in this work were performed adiabatically, or without thermostating. No periodic boundary conditions were used during any phase

of the simulations, which were performed using the Sandia-developed code Warp.<sup>27,28</sup>

**Results.** We first illustrate the stress-induced B2 to BCT phase transformation, which is shown in Figure 1 for a deformation temperature of 350 K. The zero strain snapshot in Figure 1 corresponds to the energy-minimized positions of the initially ideal B2 lattice; the energy minimization leads to an approximately 7% contraction in nanowire length due to the inherently tensile surface stresses. Upon application of tensile loading, the phase transformation occurs heterogeneously along the length of the wire and is illustrated by the snapshots at  $\epsilon = 0.09$  and 0.23 in Figure 1. All unit cells within the wire have transformed from B2 to BCT at a strain of 38%.

A simple crystallographic discussion is required to verify the martensitic phase transformation. As previously mentioned, the original B2 lattice is cubic with a lattice parameter of 0.28712 nm. The stress-induced martensitic phase transformation to the BCT phase results in the new lattice parameters of  $a = 0.26$  nm and  $c = 0.373$  nm, which corresponds to expansion of the wire in the  $x$ -direction due to the applied load and a corresponding contraction in the  $y$ - and  $z$ -directions. These values were obtained by considering the positions of a unit cell in the interior of the nanowire as to mitigate surface effects on the unit cell distortion and were calculated by an average of all atomic coordinates in each direction. Snapshots of the initially cubic B2 lattice and the resulting BCT lattice after the stress-induced phase transformation are shown in Figure 2.

The stress–strain curves for the initially B2 NiAl nanowires across a range of deformation temperatures are shown in Figure 3. The first observable trend is that the strain at which the initially B2 nanowire has completely phase-transformed to the BCT phase decreases with increasing temperature. The phase transformation finishes during the second phase of linear elastic deformation in the stress–strain curve and begins at a strain of about  $\epsilon = 0.39$  at 50

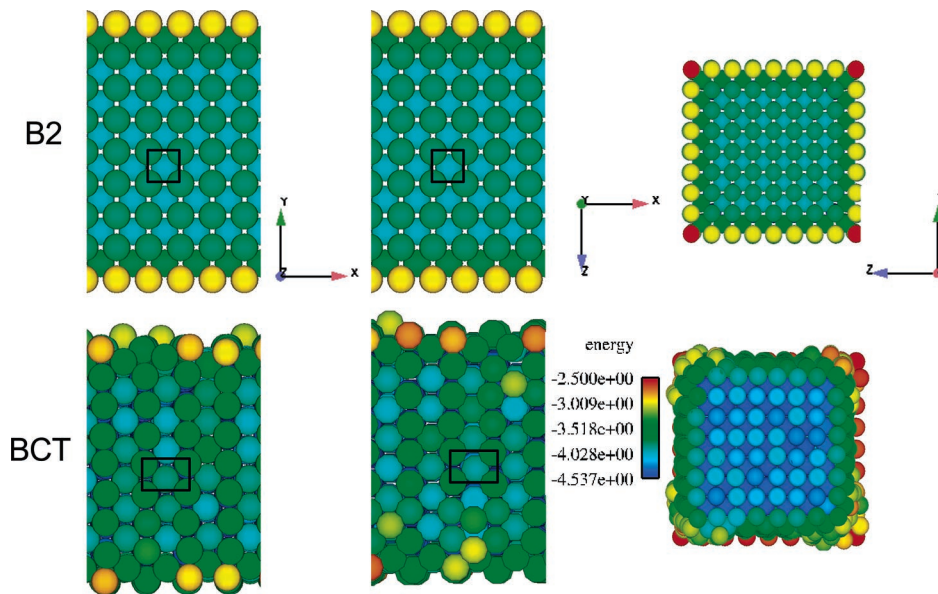


**Figure 2.** Configurations of the wire in the initial B2 phase (top) followed by the stress-induced BCT phase (bottom).

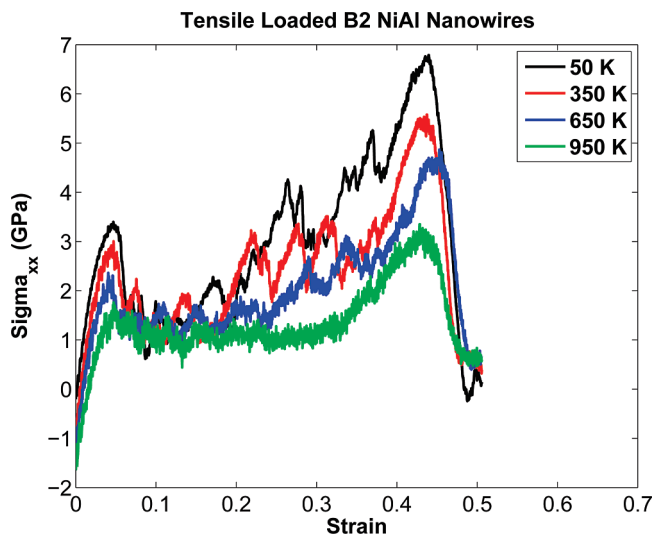


**Figure 3.** Stress–strain curves for the initially B2 NiAl nanowire at various deformation temperatures.

K, while the nanowire at 950 K has completely transformed to BCT at a strain of about  $\epsilon = 0.36$ . The reason for this will be discussed later.

We note three additional trends of interest. First, the tangent modulus of the linear elastic deformation after the phase transformation to BCT has occurred decreases with temperature, demonstrating the effect of thermally induced softening in elastic nanoscale deformation. Second, the stress plateau after the transformation stress is reached becomes flatter at higher temperatures; the transformation stress corresponds to the stress peak after the initial linear elastic deformation in Figure 3. This point and the fact that the transformation stress shows a peak relative to the stress during the resulting plateau are related to the heterogeneous nature of the phase transformation at lower temperatures and will be discussed below. Finally, it is interesting that the strain that the nanowires can sustain before yielding occurs is about 43%, while the fracture strain at 950 K is about 56%. By

comparison, recent calculations using density functional theory indicate that the ideal tensile strain, or the upper limit of deformation a material can never exceed, for a B2 NiAl lattice in the  $\langle 100 \rangle$  direction is about 58%.<sup>17</sup>

As mentioned above, the stress plateaus in Figure 3 following the transformation stress show differing behavior depending on the deformation temperature. At lower temperatures, the stress generally increases following the transformation stress; however, at 950 K, the stress following the transformation stress remains relatively constant at about 1 GPa from strains of about  $\epsilon = 0.04$  to  $\epsilon = 0.33$ . In polycrystalline shape memory alloys<sup>18</sup>, the relatively constant period of stress with increasing strain following the transformation stress occurs due to the initiation of the austenite to martensite phase transformation. Once the phase transformation is complete, the resulting martensite phase can deform in an essentially linear elastic fashion until yielding via irreversible slip occurs.

A similar trend with certain key differences is observed in the intermetallic NiAl nanowires. At low temperatures, the phase transformation of the NiAl nanowire from B2 to BCT occurs heterogeneously through the nucleation, propagation, and annihilation of multiple  $\{101\}$  twinning planes. This is illustrated in Figure 4, which shows the detwinning process within a small subsection of the wire at 50 K. The top snapshot in Figure 4a shows two planes of B2 unit cells separated by  $\{101\}$  twinning planes that have not undergone the phase transformation. The bottom snapshot in Figure 4a illustrates that rotating the wire  $90^\circ$  about its longitudinal axis shows the  $\{101\}$  twinning planes separating the untransformed B2 unit cells and the transformed BCT unit cells. Figure 4b illustrates that under further loading one plane of B2 unit cells has undergone the phase transformation, leaving one untransformed plane of unit cells. Therefore, in the bottom image in Figure 4b, there exists only one  $\{101\}$  twinning plane separating the B2 and BCT phases in the nanowire.

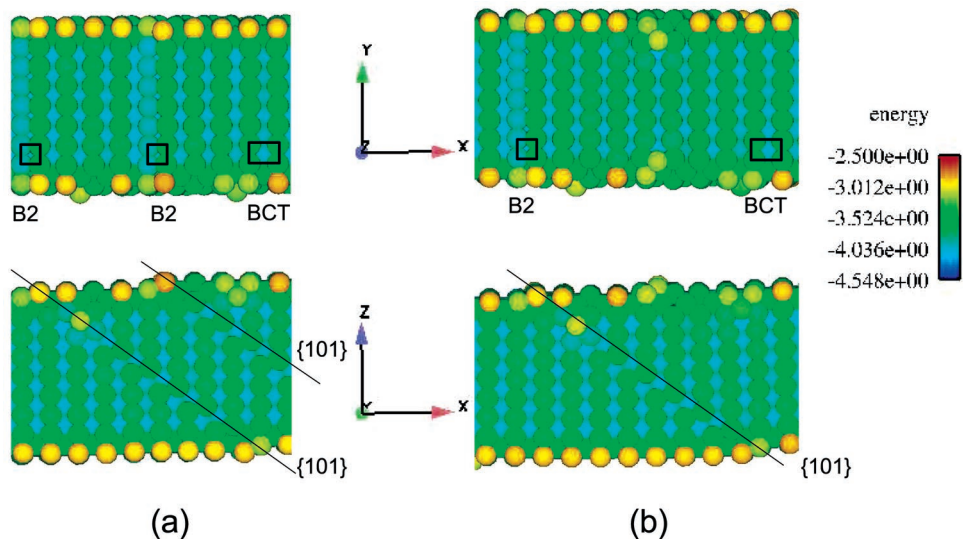


**Figure 4.** Closeup view of the  $\{101\}$  twinning planes separating the B2 and BCT phases during the stress-induced martensitic phase transformation at 50 K.

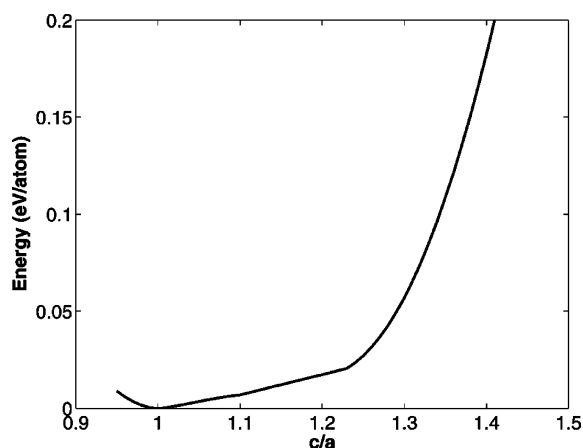


**Figure 5.** Energy as a function of the tetragonal ratio  $c/a$  along the Bain path for the Voter–Chen NiAl potential.  $c/a = 1$  corresponds to the ideal B2 lattice, while  $c/a = \sqrt{2}$  corresponds to the BCT phase.

At 950 K, instead of heterogeneous phase transformation occurring along the length of the wire, a single  $\{101\}$  twinning plane propagates through the wire under the applied tensile loading. This more uniform phase transformation explains the constant stress plateau following the transformation stress at 950 K as well as the difference in transformation strain when the BCT phase is reached. Because of the long-ranged nature of the stress fields in the wire due to the twinning planes, the heterogeneous nucleation of multiple  $\{101\}$  twinning planes at lower temperatures results in the interactions of these long-ranged stress fields and increases the amount of stress and strain that is necessary during the phase transformation to drive together and annihilate the twinning planes. At 950 K, once the  $\{101\}$  twinning plane has been nucleated, the same stress state is required to propagate the twinning plane as there are no interactions with other propagating twinning planes, resulting in a flat stress plateau. In addition, the peak in the transformation stress at lower temperatures occurs for a similar reason; that is, a

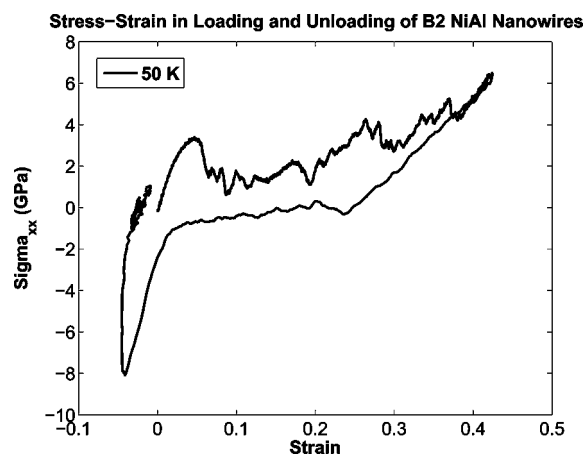


**Figure 6.** Loading and unloading stress–strain curve for NiAl nanowire at 50 K illustrating pseudoelastic recovery of inelastic strain.

larger stress is required to initiate the phase transformation due to the heterogeneous nature of the nucleation.

The stability of the resultant BCT phase was investigated by unloading the nanowires after complete transformation to the BCT phase had occurred. Ab initio calculations of the deformation of an initially B2 NiAl lattice along the volume-preserving Bain path indicate that the BCT phase is unstable for NiAl.<sup>29,30</sup> However, a metastable BCT phase has been experimentally reported for NiAl by Schryvers and Ma<sup>31</sup>. The energetics of the Voter–Chen potential utilized in this work were tested by calculating the potential energy of a bulk NiAl system by varying the tetragonal ratio  $c/a$  along the volume-conserving Bain deformation path. As shown in Figure 5, the energy is minimized for  $c/a = 1$ , which corresponds to an ideal, undeformed B2 lattice. In contrast, the potential energy of the system gradually increases with increasing tetragonal distortion, illustrating the instability of the resulting BCT phase at  $c/a = \sqrt{2}$  and showing agreement with the previously discussed ab initio calculations.<sup>29,30</sup>

This instability was verified by unloading the nanowires after the stress-induced martensitic phase transformation from B2 to BCT. The unloading resulted in instability of the BCT phase, as the nanowires at all deformation temperatures contracted to the initial B2 phase. This is illustrated for the NiAl nanowire at 50 K in Figure 6, which shows the recovery of inelastic strains on the order of 40%, which greatly exceeds previously observed amounts of approximately 10% in bulk, polycrystalline SMAs such as NiTi;<sup>18</sup> similar predictions have been obtained for monatomic shape memory metal nanowires.<sup>9,11</sup> The large amount of hysteresis in compression occurs due to dynamic effects and the rate of contraction during the unloading process.

In conclusion, intermetallic B2 NiAl nanowires have been shown to undergo a stress-induced martensitic phase transformation to a BCT phase. The phase transformation proceeds heterogeneously by propagation and annihilation of multiple {101} twinning planes at lower temperatures and a single {101} twinning plane at elevated temperatures, leading to disparate post-transformation stress behavior at different temperatures. The instability of the BCT phase was shown both through direct calculation of the system energetics as well as by unloading the nanowires after the stress-induced phase transformation from B2 to BCT had occurred; this results in pseudoelastic recovery of inelastic strains on the order of 40% at all deformation temperatures.

**Acknowledgment.** H.S.P. gratefully acknowledges startup funding from Vanderbilt University in support of this research.

## References

- (1) Lieber, C. M. *MRS Bull.* **2003**, 28 (7), 486–491.
- (2) Yang, P. *MRS Bull.* **2005**, 30 (2), 85–91.
- (3) Cammarata, R. C. *Prog. Surf. Sci.* **1994**, 46 (1), 1–38.
- (4) Gall, K.; Diao, J.; Dunn, M. L. *Nano Lett.* **2004**, 4 (12), 2431–2436.
- (5) Park, H. S.; Zimmerman, J. A. *Phys. Rev. B* **2005**, 72, 054106.
- (6) Diao, J.; Gall, K.; Dunn, M. L. *Nano Lett.* **2004**, 4 (10), 1863–1867.
- (7) Park, H. S.; Gall, K.; Zimmerman, J. A. *J. Mech. Phys. Solids* **2005**.
- (8) Diao, J.; Gall, K.; Dunn, M. L. *Nat. Mater.* **2003**, 2 (10), 656–660.
- (9) Park, H. S.; Gall, K.; Zimmerman, J. A. *Phys. Rev. Lett.* **2005**, 95, 255504.
- (10) Liang, W.; Zhou, M. *J. Eng. Mater. Technol.* **2005**, 127 (4), 423–433.
- (11) Liang, W.; Zhou, M.; Ke, F. *Nano Lett.* **2005**, 5 (10), 2039–2043.
- (12) George, E. P.; Yamaguchi, M.; Kumar, K. S.; Liu, C. T. *Annu. Rev. Mater. Sci.* **1994**, 24, 409–451.
- (13) George, E. P.; Liu, C. T.; Horton, J. A.; Sparks, C. J.; Kao, M.; Kunsmann, H.; King, T. *Mater. Charact.* **1997**, 39, 665–686.
- (14) Jee, K. K.; Potapov, P. L.; Song, S. Y.; Shin, M. C. *Scr. Mater.* **1997**, 36 (2), 207–212.
- (15) Nagasawa, A.; Enami, K.; Ishino, Y.; Abe, Y.; Nenno, S. *Scr. Metall.* **1974**, 8, 1055–1060.
- (16) Kim, Y. D.; Wayman, C. M. *Scr. Metall. Mater.* **1990**, 24 (2), 245–250.
- (17) Li, T.; Morris, J. W.; Chrzan, D. C. *Phys. Rev. B* **2004**, 70, 054107.
- (18) Otsuka, K.; Ren, X. *Prog. Mater. Sci.* **2005**, 50, 511–678.
- (19) Rubini, S.; Ballone, P. *Phys. Rev. B* **1993**, 48 (1), 99–111.
- (20) Ye, Y. Y.; Chan, C. T.; Ho, K. M.; Wang, C. Z. *Phys. Rev. B* **1994**, 49 (9), 5852–5857.
- (21) Shao, Y.; Clapp, P. C.; Rifkin, J. A. *Metall. Mater. Trans. A* **1996**, 27, 1477–1489.
- (22) Meyer, R.; Entel, P. *Comput. Mater. Sci.* **1998**, 10, 10–15.
- (23) Chen, S. P.; Voter, A. F.; Srolovitz, D. J. *Phys. Rev. Lett.* **1986**, 57 (11), 1308–1311.
- (24) Voter, A. F.; Chen, S. P. *Mater. Res. Soc. Symp. Proc.* **1987**, 82, 175–180.
- (25) Nosé, S. *J. Chem. Phys.* **1984**, 81, 511–519.
- (26) Hoover, W. G. *Phys. Rev. A* **1985**, 31, 1695–1697.
- (27) Plimpton, S. J. *J. Comput. Phys.* **1995**, 117, 1–19.
- (28) *Warp*; Sandia National Laboratories: Albuquerque, NM, 2005. <http://www.cs.sandia.gov/~sjplimp/lammmps.html>.
- (29) Mishin, Y.; Mehl, M. J.; Papaconstantopoulos, D. A. *Phys. Rev. B* **2002**, 65, 224114.
- (30) Takizawa, S.; Miura, S.; Mohri, T. *Intermetallics* **2005**, 13, 1137–1140.
- (31) Schryvers, D.; Ma, Y. *J. Alloys Compd.* **1995**, 221, 227–234.

NL060024P